Nanodiamond Analysis Methods Compared for Consistency. J. B. Lewis[1,2], D. Isheim[4], C. Floss[1,2], T. L. Daulton[2,3], D. N. Seidman[4], [1]Laboratory for Space Sciences, [2]Physics Dept., Washington University, [3]Institute of Materials Science and Engineering, St. Louis, MO. Email: jblewis@go.wustl.edu. [4]Center for Atom-Probe Tomography, Dept. of Materials Science and Engineering, Northwestern University, Evanston, IL.

Introduction: The origins of meteoritic nanodiamonds (NDs) remain an enigma. Isotopic anomalies in trace elements, such as Xe [1], Te [2], Pa [3], and Ba [4] suggest a Type II supernova origin for at least a subpopulation of the NDs. While the bulk measured C [5] and N [6] are consistent with formation in the Solar System, bulk measurements are not diagnostic. Poorly-crystalline to amorphous carbonaceous phases, which can comprise a significant fraction of the residue [7], are potentially of different origin than the nanodiamonds and hence can have different C isotopic compositions. To resolve this conundrum efforts are ongoing to measure the $^{12}C/^{13}C$ ratio of individual ND grains using atom-probe tomography (APT) [8]. APT achieves high accuracy for measurements of elemental concentration in many materials, but some "high field" materials, including C, are known to yield biased isotopic ratios prior to correction [8, 9]. In the absence of any standardized peak fitting technique it is necessary to ensure that results obtained by different investigators are reproducible. We compare two analysis procedures, one from [9], and one introduced herein and used to analyze nine new detonation nanodiamond standards (DND) and three meteoritic nanodiamond residue samples from the Allende DM separate (ADM).

Experimental: A full description of specimen preparation is given in [8, 10]. After focused ion-beam microscope liftout, APT of nanodiamonds embedded between sputter-deposited Pt layers was performed with a Cameca LEAP 4000X Si [8, 10], yielding 3D positions and time-of-flight data for ~57% of the atoms (i.e., collection yield) in needle-shaped sample nanotips of radius 20–100 nm. High ultraviolet laser pulse energies (i.e., a large fraction of the energy required to remove ions from the sample surface is provided by laser pulsing rather than a standing dc voltage) must be used to reduce the probability of nanotip fracture, but these lead to more delayed evaporation events, which manifest themselves as peak-tails. Since isotopes of the same element generally have similar mass-to-charge-state (m/n) ratios, they are particularly susceptible to tail interferences. Peak shape is determined by the base temperature, length of the laser-induced thermal pulse, nanotip shape, and material properties. As a result, no standardized peak-fitting method exists for APT. In [9] the width of the region of interest for each peak to be integrated, or "range", is defined to begin and end when the peak crosses $2\times$ the background, using a 0.01 amu bin size. For this analysis method, the local noise/bin is then calculated and subtracted based on ranges on either side of each peak. For the new data we employ a different procedure: We first subtract the background as calculated by a linear fit to the baseline of the time-of-flight spectrum, and define the range as the FWHM with a bin size calibrated such that the range is covered by five bins. For minor isotopes we use the same range width as was used for the major isotope, rather than FWHM; e.g., $^{13}C^+$ is fit with the same range width as $^{12}C^+$. This is because for same-element, same-charge-state ions none of the factors affecting peak shape should vary, and the shift in time-of-flight/amu over 1 amu is negligibly small compared to bin size. Therefore, ranges are better defined by the largest peaks. Finally, for ^{13}C (+ & 2+) the contribution from the tails of ^{12}C (+ & 2+) is estimated and subtracted. This procedure is largely based on [11]. For both methods, iterative proportional fitting of detected multiple isotope pairs is used to generate a correction for signal loss due to detector deadtime [9].

Results: Mean standard ratios are plotted for old (DND1) and new (DND2) data in Fig. 1 (a), along with standard error of the mean (SEOM) and standard deviation. These data sets are combined and compared to Allende data, Fig. 1 (b). The SEOM is representative of the uncertainty in the determination of the mean value, while the standard deviation represents the scatter of the data. DND2 reproduces the significant instrumental artifact leading to an underestimation of $^{12}C/^{13}C$ ratios [8, 9]. In DND2, which was analyzed using the new procedure, the mean ratio is closer to the expected value, but the ratios measured for different charge states are further from agreement. In both cases the difference is only marginally significant. The scatter for the DND2 charge state + ratios is significantly smaller than for DND1.

Isotopic Ratios. The mean Allende ratio (for nanodiamonds and poorly-crystalline to amorphous C residuals) is, within uncertainties, the same as that of the mean standard ratio. The scatter in the charge state 2+ ratio is greater than for the standards, while the scatter in the + ratio is actually *less*, whereas we would expect a greater deviation for the ADMs if isotopically anomalous grains were present. We conclude that little if any of the carbonaceous material we have analyzed from the Allende residue is presolar. Given our current sample size, the presence of non-diamond carbonaceous material, and remaining instrumental artifacts; this conclusion should not be applied too broadly. The
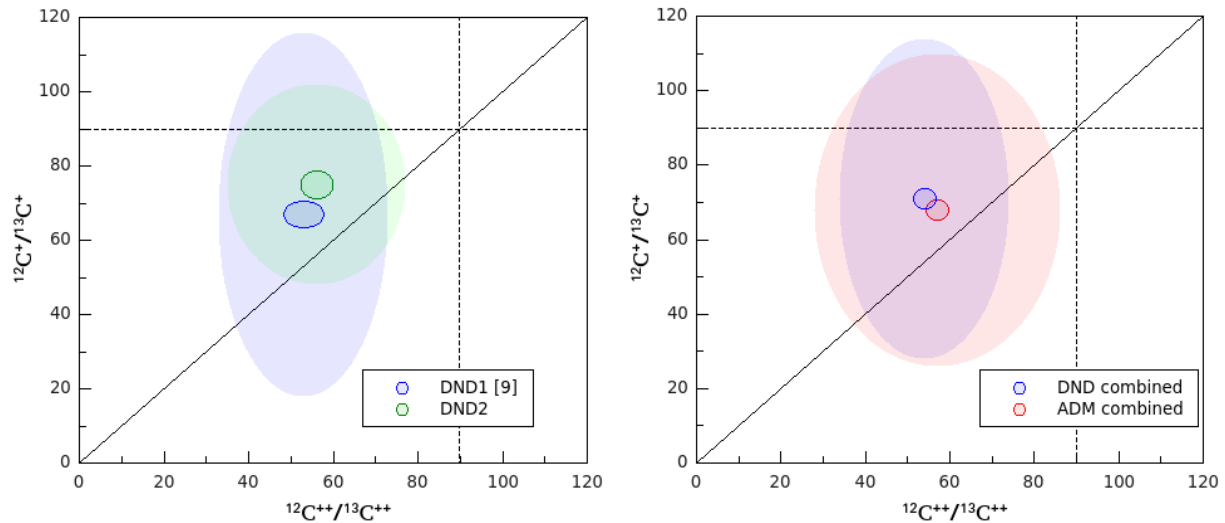
Fig. 1 (a) Mean C isotopic ratios for two sets of terrestrial nanodiamond standard data, analyzed using two different procedures. Small ovals represent $\pm 2\times$ the standard error of the mean. Large ovals represent $\pm 2\times$ the standard deviation of a datum from the mean. The diagonal line is the line of equal ratio for isotopes at the two different charge states. The horizontal and vertical lines are the expected, solar system isotopic $^{12}C/^{13}C$ ratio, 89.9. **(b)** Mean C isotopic ratios for combined terrestrial standard and combined Allende DM nanodiamond data.

mean ratio of $^{12}C/^{13}C$ in charge state + is significantly greater than in charge state 2+. There is no reason to believe the different charge states of C would have different isotopic ratios, therefore we take this difference to be the result of an experimental artifact that increases the measured $^{12}C^+$ and/or $^{13}C^{++}$ as well as possibly decreasing the measured $^{12}C^{++}$ and/or $^{13}C^+$. Undercorrection of $^{12}C^+$ or overcorrection of $^{12}C^{++}$ for deadtime effects could explain the discrepancy, as could $^{12}C_2^{++}$ interference at 12 amu. $(^{12}CH)^+$ hydride interference would give the opposite effect.

Deadtime Corrections. On average the correction to the $^{12}C^{++}$ peak is several orders of magnitude greater than to the $^{12}C^+$ peak. This feature is in agreement with the corrections made by [12] using a different method. It is well-known that smaller laser pulse energies in APT lead to preferential formation of higher charge-state ions; we therefore surmise that the detection multiplicity also increases with a smaller pulse fraction.

Na and other dissolution residuals. We detected Na and NaO in small clusters inside of large, low-density, dirty C clusters. Trace amounts of Cl, Cr, and F were also detected. Presumably these are residues from the dissolution and separation process. We have begun to reanalyze data from [9] and find evidence of Na and other dissolution residuals in some but not all data sets. This is consistent with observations of individual and clustered contaminant atoms within the poorly-crystalline to amorphous-C residue [7].

Outlook: In future work we will extend the comparison of procedures by applying the new technique to the data from [9] and the old technique to the data original to this research. We intend to survey available APT nanodiamond data to further investigate the possible connection between pulse energy and detection multiplicity as calculated by deadtime correction algorithms, to assess the effect of $^{12}C_2^{++}$ and $(^{12}CH)^+$ on C-ratio measurements, and to determine if the concentration or distribution of Na, Cr, Cl, or F vary depending on the type of C-clusters in which they are contained. Correlated transmission electron microscopy and APT of nanotips will allow us to compare the crystal structure of the C residue with the reconstructed m/n data, and allow us to distinguish between nanodiamond and amorphous C phases

References: [1] Lewis R. S. et al. (1987) *Nature 326*, 160–162. [2] Richter S. et al. (1998) *Nature 391*, 261–263. [3] Maas R. et al. (2001) *Meteorit. Planet. Sci. 36*, 849–858. [4] Lewis R. S. et al. (1991) *LPS XXII*, 807–808. [5] Russell S. R. et al (1996) *Meteorit. Planet. Sci. 31*, 343–355. [6] Marty B. et al. (2011), *Science 332*, 1533–1536. [7] Stroud R. M. et al. (2011) *ApJL, 738*, L27–L31. [8] Heck P. R. et al. (2014) *Meteorit. Planet. Sci. 49* (3) 453–467. [9] Lewis J. B. et al. (2015, *submitted*) *Ultramicroscopy*. [10] Isheim D. et al. (2013) *Microsc. Microanal., 19* (Suppl 2), CD974–CD975. [11] Hudson D. et al. (2011) *Ultramicroscopy, 111*, 480–486. [12] Stephan T. et al. (2015, *in press*) *Int. J Mass Spectrom.*